

Equation of State for supernova explosion simulations

D.P.Menezes¹ and C. Providência²

¹*Depto de Física - CFM - Universidade Federal de Santa Catarina Florianópolis - SC - CP. 476 - CEP 88.040 - 900 - Brazil*

²*Centro de Física Teórica - Dep. de Física - Universidade de Coimbra - P-3004 - 516 Coimbra - Portugal*

In this work we present a detailed explanation of the construction of an appropriate equation of state (EoS) for nuclear astrophysics. We use a relativistic model in order to obtain an EoS for neutrally charged matter that extends from very low to high densities, from zero temperature to 100 MeV with proton fractions ranging from 0 (no protons) to 0.6 (asymmetric matter with proton excess). For the achievement of complete convergence, the Sommerfeld approximation is used at low temperatures and the Boltzman distribution for relativistic particles is used in the calculation of the electron properties at very low densities. Photons are also incorporated as blackbody radiation. An extension of this EoS is also presented with the inclusion of strangeness by taking into account the Σ^- hyperon only. Strangeness fractions range from 0.02 to 0.3.

I. INTRODUCTION

The observed pulsars, also commonly known as neutron stars, are believed to be the remnants of type II supernova explosions. These type II supernovae appear at the end of the evolution of very massive stars. The core of these stars collapses to a density around several times nuclear saturation density. A rebound takes place and drives a shockwave which expells most of the original mass of the star. The simulation of supernova explosions and the conditions for them to take place have been subject of investigation for the last 30 years. Depending on certain thermodynamical conditions present in the equations of state (EoS), the supernova explosion simulation is successful or not [1]. The EoS built for nuclear astrophysics purposes depends on a series of thermodynamic properties which are obtained for certain temperatures, densities and matter composition. Hence, an efficient EoS which is reasonably accurate is mandatory for a supernova explosion simulation to be successful.

In order to obtain an equation of state (EoS) for low and high density matter suitable to astrophysical applications, the relativistic non linear Walecka model (NLWM) [2, 3] is used. For matter to be neutral, electrons are also included. For sufficiently high densities the formation of hyperons is energetically favored. Normally, the appearance of the strange baryons softens the EoS. Our formalism is described next with the inclusion of the whole baryonic octet for the sake of completeness but, in a first step towards a complete description of a supernova explosion, only protons and neutrons are considered. Next we incorporate strangeness but restrict ourselves to the inclusion of Σ^- . Convergence problems are well known to exist at low temperatures and below certain densities. Appropriate approximations are then utilized. Blackbody radiation is considered and, whenever convenient, electrons and positrons are described separately. Future prospects for obtaining more sophisticated EoS are discussed.

II. HADRONIC MATTER EQUATION OF STATE

A common extension of the NLWM considers the inclusion of the whole baryonic octet (n , p , Λ , Σ^+ , Σ^0 , Σ^- , Ξ^- , Ξ^0) in the place of the nucleonic sector. In this work we present the complete formalism, but numerical calculations were performed with nucleons only.

The lagrangian density of the NLWM reads:

$$\mathcal{L} = \mathcal{L}_B + \mathcal{L}_{mesons} + \mathcal{L}_{leptons}, \quad (1)$$

where

$$\mathcal{L}_B = \sum_B \bar{\psi}_B [\gamma_\mu (i\partial^\mu - g_{vB}V^\mu - g_{\rho B}\mathbf{t} \cdot \mathbf{b}^\mu) - (M_B - g_{sB}\phi)] \psi_B,$$

with \sum_B extending over the chosen baryons B,

$$g_{sB} = x_{sB} g_s, \quad g_{vB} = x_{vB} g_v, \quad g_{\rho B} = x_{\rho B} g_\rho$$

and x_{sB} , x_{vB} and $x_{\rho B}$ are equal to 1 for the nucleons and acquire different values in different parametrizations for the other baryons,

$$\mathcal{L}_{mesons} = \frac{1}{2}(\partial_\mu \phi \partial^\mu \phi - m_s^2 \phi^2) - \frac{1}{3!}\kappa \phi^3 - \frac{1}{4!}\lambda \phi^4 - \frac{1}{4}\Omega_{\mu\nu}\Omega^{\mu\nu} + \frac{1}{2}m_v^2 V_\mu V^\mu$$

$$-\frac{1}{4}\mathbf{B}_{\mu\nu} \cdot \mathbf{B}^{\mu\nu} + \frac{1}{2}m_\rho^2 \mathbf{b}_\mu \cdot \mathbf{b}^\mu, \quad (2)$$

where $\Omega_{\mu\nu} = \partial_\mu V_\nu - \partial_\nu V_\mu$, $\mathbf{B}_{\mu\nu} = \partial_\mu \mathbf{b}_\nu - \partial_\nu \mathbf{b}_\mu - g_\rho(\mathbf{b}_\mu \times \mathbf{b}_\nu)$ and \mathbf{t} is the isospin operator.

In the above lagrangian, neither pions nor kaons are included because they vanish in the mean field approximation which is used in the present work and we do not consider the possible contribution of pion and kaon condensates. The leptonic sector is included as a free fermi gas which does not interact with the hadrons. Its lagrangian density reads:

$$\mathcal{L}_{leptons} = \sum_l \bar{\psi}_l (i\gamma_\mu \partial^\mu - m_l) \psi_l. \quad (3)$$

In the present work only electrons (and positrons are considered). In the mean field approximation (MFA) (see [4, 5], for instance), the meson equations of motion read:

$$\phi_0 = -\frac{\kappa}{2m_s^2}\phi_0^2 - \frac{\lambda}{6m_s^2}\phi_0^3 + \sum_B \frac{g_s}{m_s^2} x_{sB} \rho_{sB}, \quad (4)$$

$$V_0 = \sum_B \frac{g_v}{m_v^2} x_{vB} \rho_B, \quad (5)$$

$$b_0 = \sum_B \frac{g_\rho}{m_\rho^2} x_{\rho B} t_{3B} \rho_B, \quad (6)$$

with

$$\rho_B = 2 \int \frac{d^3p}{(2\pi)^3} (f_{B+} - f_{B-}), \quad \rho = \sum_B \rho_B, \quad (7)$$

$$\rho_{sB} = \frac{1}{\pi^2} \int p^2 dp \frac{M_B^*}{\sqrt{p^2 + M_B^{*2}}} (f_{B+} + f_{B-}),$$

with $M_B^* = M_B - g_{sB} \phi$, $B\pm$ stands respectively for baryons and anti-baryons, t_{3B} is the third component of the baryon isospin, $E^*(\mathbf{p}) = \sqrt{\mathbf{p}^2 + M^{*2}}$ and

$$f_{B\pm} = 1/\{1 + \exp[(E^*(\mathbf{p}) \mp \nu_B)/T]\}, \quad (8)$$

where the effective chemical potential is

$$\nu_B = \mu_B - g_{vB} V_0 - g_{\rho B} t_{3B} b_0. \quad (9)$$

Within the MFA, the meson fields are taken as classical fields whilst the baryon fields remain quantum [2]. On the other hand, the Dirac equation, which is the equation of motion for the baryons is not solved directly but instead used in the calculation of the densities appearing in the meson equations of motion. The system has then to be solved self-consistently.

At $T = 0$, the distribution functions for baryons are replaced by step functions. In this case equation (7) becomes simply $\rho_B = k_{FB}^3/3\pi^2$. The baryonic energy density in the mean field approximation reads:

$$\begin{aligned} \mathcal{E}_B = & 2 \sum_B \int \frac{d^3p}{(2\pi)^3} \sqrt{\mathbf{p}^2 + M^{*2}} (f_{B+} + f_{B-}) + \\ & \frac{m_s^2}{2}\phi_0^2 + \frac{\kappa}{6}\phi_0^3 + \frac{\lambda}{24}\phi_0^4 + \frac{m_v^2}{2}V_0^2 + \frac{\xi g_v^4}{8}V_0^4 + \frac{m_\rho^2}{2}b_0^2 \end{aligned} \quad (10)$$

and the related pressure becomes

$$\begin{aligned} P_B = & \frac{1}{3\pi^2} \sum_B \int dp \frac{\mathbf{p}^4}{\sqrt{\mathbf{p}^2 + M^{*2}}} (f_{B+} + f_{B-}) \\ & - \frac{m_s^2}{2}\phi_0^2 - \frac{\kappa\phi_0^3}{6} - \frac{\lambda\phi_0^4}{24} + \frac{m_v^2}{2}V_0^2 + \frac{\xi g_v^4 V_0^4}{24} + \frac{m_\rho^2}{2}b_0^2. \end{aligned} \quad (11)$$

The entropy of the baryons are taken as

$$\begin{aligned} \mathcal{S}_B = & -2 \sum_B \int \frac{d^3 p}{(2\pi)^3} [f_{B+} \log(f_{B+}) + (1 - f_{B+}) \log(1 - f_{B+}) \\ & + f_{B-} \log(f_{B-}) + (1 - f_{B-}) \log(1 - f_{B-})] \end{aligned} \quad (12)$$

and hence the free energy reads

$$\mathcal{F}_B = \mathcal{E}_B - T\mathcal{S}_B. \quad (13)$$

Notice again that the above expressions were obtained for finite temperature, but they can be easily modified for $T = 0$. Whenever $T=0$, no anti-particles are present.

At very low T ($-0.4 \leq \log(T) < -0.1$ MeV) there are well known convergence problems due to the distribution functions and in this case we use the Sommerfeld approximation for the baryons [6]. The effective chemical potentials, in particular, read

$$\nu_i = \epsilon_{Fi} - \frac{\pi^2}{6} T^2 \frac{(k_{Fi}^2 + \epsilon_{Fi}^2)}{k_{Fi} \epsilon_{Fi}}, \quad i = p, n. \quad (14)$$

For the net electron density we have

$$\rho_e = 2 \int \frac{d^3 p}{(2\pi)^3} (f_{e^-} - f_{e^+}), \quad (15)$$

where the distribution functions for the particles (e^-) and antiparticles (e^+) are given by

$$f_{e^\mp} = 1/(1 + \exp[(\epsilon \mp \mu_e)/T]), \quad (16)$$

with μ_e as the chemical potential. In order to ensure charge neutrality, electron and proton densities have to be equal, i.e.,

$$\rho_e = \rho_p. \quad (17)$$

Next we always distinguish between electrons (e^-) and positrons (e^+) and when both particles and antiparticles are considered we refer to the related quantity with the index e . At $T = 0$, the distribution functions for the leptons are also replaced by step functions and no positrons are left. In this case equation (15) becomes simply $\rho_e = k_{Fe}^3/3\pi^2$. The thermodynamic quantities read

$$\mathcal{E}_e = 2 \int \frac{d^3 p}{(2\pi)^3} \sqrt{\mathbf{p}^2 + m_e^2} (f_{e^-} + f_{e^+}), \quad (18)$$

$$\mathcal{E}_{e^-} = 2 \int \frac{d^3 p}{(2\pi)^3} \sqrt{\mathbf{p}^2 + m_e^2} f_{e^-}, \quad \mathcal{E}_{e^+} = 2 \int \frac{d^3 p}{(2\pi)^3} \sqrt{\mathbf{p}^2 + m_e^2} f_{e^+}, \quad (19)$$

$$P_e = \frac{1}{3\pi^2} \int \frac{\mathbf{p}^4 dp}{\sqrt{\mathbf{p}^2 + m_e^2}} (f_{e^-} + f_{e^+}), \quad (20)$$

$$P_{e^-} = \frac{1}{3\pi^2} \int \frac{\mathbf{p}^4 dp}{\sqrt{\mathbf{p}^2 + m_e^2}} f_{e^-}, \quad P_{e^+} = P_e - P_{e^-} \quad (21)$$

$$\mathcal{S}_e = \frac{\mathcal{E}_e + P_e - \mu_e \rho_e}{T}, \quad \mathcal{S}_{e^-} = \frac{\mathcal{E}_{e^-} + P_{e^-} - \mu_e \rho_{e^-}}{T}, \quad \mathcal{S}_{e^+} = \frac{\mathcal{E}_{e^+} + P_{e^+} + \mu_e \rho_{e^+}}{T}, \quad (22)$$

$$\mathcal{F}_e = \mathcal{E}_e - T\mathcal{S}_e, \quad \mathcal{F}_{e^-} = \mathcal{E}_{e^-} - T\mathcal{S}_{e^-}, \quad \mathcal{F}_{e^+} = \mathcal{E}_{e^+} - T\mathcal{S}_{e^+}, \quad (23)$$

The particle fraction is defined as $y_i = \rho_i/\rho$, where $i = p, n, e^-, e^+$, and ρ is the total baryonic density.

At very low densities a Boltzman distribution for relativistic electrons and positrons is necessary [7]. The low density limit depends on the temperature and is numerically chosen such that eqs. (15) and (17) are equal within a 10^{-6} precision. If the difference is larger than this limit, eq. (17) is chosen and the corresponding chemical potentials are

$$\nu_e = m_e + \log \left[\frac{\rho_e}{g} \left(\frac{2\pi}{Tm_e} \right)^{3/2} \right], \quad (24)$$

with $g = 2$ defined as the spin multiplicity, Moreover,

$$\rho_e = (e^{\mu_e/T} - e^{-\mu_e/T}) \frac{I_1}{\pi^2}, \quad (25)$$

or analogously,

$$\mu_e = T \log \left[\frac{z}{2} + \sqrt{\frac{z^2}{4} + 1} \right], \quad z = \pi^2 \rho_e / I_1. \quad (26)$$

The energy density and pressure become

$$\mathcal{E}_e = (e^{\mu_e/T} - e^{-\mu_e/T}) \frac{I_2}{\pi^2}, \quad (27)$$

$$P_e = (e^{\mu_e/T} - e^{-\mu_e/T}) \frac{(I_2 - m_e^2 I_0)}{3\pi^2}, \quad (28)$$

where $\beta = 1/T$, $I_0 = \frac{m_e}{\beta} K_1(m_e \beta)$, $I_1 = -\frac{dI_0}{d\beta} = \frac{m_e}{\beta^2} K_1(y) - \frac{m_e^2}{\beta} \frac{dK_1}{dy}$, $I_2 = -\frac{dI_1}{d\beta} = \frac{2m_e}{\beta^3} K_1(y) - 2\frac{m_e^2}{\beta^2} \frac{dK_1}{dy} + \frac{m_e^3}{\beta} \frac{d^2 K_1}{dy^2}$, with $y = m_e \beta$, K_i are modified Bessel functions and $K'_\nu(x) = -\frac{1}{2}(K_{\nu-1}(x) + K_{\nu+1}(x))$.

The photons are taken into account via blackbody radiation and the main expressions are

$$P_\gamma = \frac{\pi^2 T^4}{45}, \quad \mathcal{S}_\gamma = \frac{4P_\gamma}{T}, \quad \mathcal{E}_\gamma = 3P_\gamma, \quad \mathcal{F}_\gamma = \mathcal{E}_\gamma - T\mathcal{S}_\gamma. \quad (29)$$

For the hadron phase we have used the GM3 parametrization proposed by Glendenning and Moszkowski [8], corresponding to an effective mass $M^* = 0.78 M$ and incompressibility $K = 240$ MeV at the saturation density $\rho_0 = 0.153 \text{ fm}^{-3}$. The coupling constants are $\left(\frac{g_s}{m_s}\right)^2 = 9.927$, $\left(\frac{g_v}{m_v}\right)^2 = 4.82$, $\left(\frac{g_\rho}{m_\rho}\right)^2 = 4.79$, $\kappa = 0.017318 g s^3$, $\lambda = -0.014526 g s^4$.

In our codes the inputs are the temperature, proton fraction and baryonic density. The grids for these quantities are $-0.4 \leq \log(T) \leq 2$ (MeV) with mesh intervals of 0.1, $0 \leq y_p \leq 0.6$ with mesh intervals of 0.02, $3 \leq \log(\rho) \leq 15.7$ (g/cm³).

In the output we have $y_p, y_n, y_{e^-}, y_{e^+}, y_e$, $\mu_p - M$ (MeV), $\mu_n - M$ (MeV), $\mu_e - m_e$ (MeV), $-\mu_e + m_e$ (MeV), \mathcal{E}_B (erg/g), \mathcal{E}_{e^-} (erg/g), \mathcal{E}_{e^+} (erg/g), \mathcal{E}_γ (erg/g), $\mathcal{E}_B + \mathcal{E}_e + \mathcal{E}_\gamma$ (erg/g), \mathcal{S}_B (k_B /baryon), \mathcal{S}_{e^-} (k_B /baryon), \mathcal{S}_{e^+} (k_B /baryon), \mathcal{S}_γ (k_B /baryon), $\mathcal{S}_B + \mathcal{S}_e + \mathcal{S}_\gamma$ (k_B /baryon), P_B (dyne/cm²), P_{e^-} (dyne/cm²), P_{e^+} (dyne/cm²), P_γ (dyne/cm²), $P_B + P_e + P_\gamma$ (dyne/cm²), $\mathcal{F}_B + \mathcal{F}_e + \mathcal{F}_\gamma$ (MeV/fm³).

III. THRESHOLD DENSITY FOR MATTER WITH STRANGENESS

To include strangeness in the EoS, Σ^- was first chosen because in β -equilibrium matter at zero temperature and with the GM3 parametrization, its onset appears at lower densities than the onset of the least massive hyperon, the Λ . Depending on the parametrization chosen for the NLWM and on the hyperon-meson coupling constants, this trend may change at higher temperatures and hence, in a future work Σ^- and Λ should be included simultaneously.

In compact stars, stellar matter is in chemical equilibrium, which means that

$$\mu_{\Sigma^0} = \mu_{\Xi^0} = \mu_\Lambda = \mu_n, \quad \mu_{\Sigma^-} = \mu_{\Xi^-} = \mu_n + \mu_e, \quad \mu_{\Sigma^+} = \mu_p = \mu_n - \mu_e.$$

In an explosive environment like the one existing in a supernova, chemical equilibrium is not supposed to be enforced. However, we consider that the time during which the supernova explosion occurs is much longer than the characteristic time of the weak interaction in such a way that the strangeness fraction is expected to be finite.

In order to build an EoS containing strangeness and appropriate for a supernova simulation we define for each energy density, temperature and proton fraction a threshold density above which a given fraction of strangeness, y_s , is allowed to exist. We determine the threshold density from the condition of β -equilibrium for the Σ^- , which is imposed through the two independent chemical potentials (μ_n and μ_e). In this case, at $T = 0$, the corresponding effective chemical potential and density are

$$\nu_{\Sigma^-} = \sqrt{k_{F\Sigma}^2 + M_{\Sigma}^{*2}} = \mu_{\Sigma^-} - g_{v\Sigma}V_0 + g_{\rho\Sigma}b_0,$$

and

$$\rho_{\Sigma} = \frac{k_{F\Sigma}^2}{3\pi^2}.$$

If the condition

$$\frac{\rho_{\Sigma}}{\rho} \geq y_s,$$

is satisfied, the appearance of the strangeness fraction y_s in the EoS is allowed. For $y_s > 0$, we define

$$\rho = \rho_n + \rho_p + \rho_{\Sigma}$$

with

$$\rho_p = y_p(1 - y_s)\rho, \quad \rho_n = (1 - y_p)(1 - y_s)\rho, \quad \rho_{\Sigma} = y_s\rho.$$

For charge neutrality,

$$\rho_e = \rho_p - \rho_{\Sigma^-} \quad (30)$$

is required.

In order to fix the meson-hyperon coupling constants we have used the prescription given in [8, 9], where the hyperon coupling constants are constrained by the binding of the Λ hyperon in nuclear matter, hypernuclear levels and neutron star masses ($x_{s\Sigma} = 0.7$ and $x_{v\Sigma} = x_{\rho\Sigma} = 0.783$) and assumed that the couplings to the Σ are equal to those of the Λ hyperon.

IV. RESULTS AND FUTURE PROSPECTS

A comprehensive test of the thermodynamic accuracy and consistency of our EoS, as described in [10], mainly when strangeness is introduced, should be performed.

A non-homogeneous phase known as pasta phase should be considered at low densities. This non-homogeneous configuration made out of spheres, rods, bubbles or other more exotic structures, have been extensively used recently [12, 13, 14]. These structures may change the neutrino opacity in supernova matter and influence neutron star quakes and pulsar glitches. We can obtain the pasta phase by building the binodal section, and therefore obtaining the chemical potentials and densities of the gas and liquid phase in equilibrium. A very crude approximation would be to forget Coulomb interaction and take zero thickness nuclei. We can consider the matter made of liquid droplets in a gas introducing two parameters: the radius of the Wigner-Seitz cell and the radius of the nucleus (equal for protons and neutrons). One of the parameters would be fixed imposing a given particle density and the other by minimizing the free energy. These results can be improved by including the Coulomb contribution and the surface energy by hand. A Thomas-Fermi calculation can then be used to obtain the pasta phase with all fields introduced in a consistent way and the surface energy calculated from the derivatives of the fields.

α -particles can be easily incorporated in the EoS as proposed in [11]. Once the pasta phase and the α -particles are included, the EoS should then be compared with reference [15]. We are already aware of some important differences. The parametrization used in [15], known as TM1 [16] reproduces ground state properties of stable and unstable nuclei. Nevertheless, this parametrization has proven not to be adequate in the description of neutron star matter because it breaks down, giving rise to negative baryon effective masses at densities existing inside a neutron star (approximately 6 times the nuclear saturation density) when hyperons are incorporated into the EoS [17]. For this reason, we usually

choose one of the parametrizations introduced by Glendenning and collaborators [9], which give a higher nucleon effective mass at the nuclear matter saturation density and, for this reason, avoids the problem of the baryon negative masses. Moreover, according to [15], the EoS with inhomogeneities has a critical temperature $T \simeq 15$ MeV above which matter is uniform. This number certainly depends on the choice of the parameters. Based on our recent works, we would expect a smaller value for the critical temperature since for nuclear matter with no electrons (no Coulomb interaction and surface tension) the critical temperature occurs for symmetric matter just above 15 MeV. The high value obtained in [15] may be due to the way the density distributions are parametrized which give rise to very stiff surfaces for the droplets. In [13] a critical temperature of ~ 5 MeV was obtained for $y_p = 0.3$ matter and ~ 6 MeV was obtained for $y_p = 0.5$. One of our recent studies on the dynamical instabilities of npe matter also predicts lower critical temperatures, more according to the results of [13]. We do not know if the differences on the EoS due to the use of different parametrizations is more important or of the order of the magnitude of the changes included due to the explicit inclusion of a non-homogeneous phase. This should be studied.

In Fig. 1 we compare our results for the free energy obtained at three different temperatures and three different proton fractions with the results of [15]. One can see that results deviate slightly at higher densities. In Fig. 2 we plot the pressure for the same temperatures and proton fractions as in Fig 1. Again the results are very similar. In Fig. 3 we plot, once more, for the same temperatures and proton fractions, the entropy. The differences are more pronounced. While at higher temperatures (50 MeV) the curves are very similar for all proton fraction, for lower temperatures the curves are identical only for neutron matter (very low proton fraction). One should notice, however, that the trends of the curves are the same.

Finally, we comment on the definition of the internal energy: it is equal to the nucleon mass for zero density at $T=0$ MeV. For finite temperature this is no longer true because of the presence of nucleons and antinucleons. We have defined the internal energy as the energy density per number density in erg/g and in [15] the internal energy is given by the energy density per number density minus the atomic mass unit. As one can see in Fig 4, both results are in accordance once the same definition is used. A more clear comparison is done in Fig. 5 where the internal energy for homogeneous matter within TM1 is also shown, and compared with the internal energy obtained with the GM3 parametrization and the EoS of [15], also with TM1 but with the non-homogeneous phase included.

Finally, as a second step in a more refined EoS with strangeness the Λ hyperons and later the whole octet and muons should be included.

ACKNOWLEDGMENTS

This work was partially supported by CNPq(Brazil), CAPES(Brazil)/GRICES (Portugal) under project 100/03 and FEDER/FCT (Portugal) under the projects POCTI/FP/63419/2005 and POCTI/FP/63918/2005.

-
- [1] J. Cooperstein, H.A. Bethe and G.E. Brown, Nucl. Phys. **A 429**, 527 (1984).
 - [2] B.D. Serot and J.D. Walecka, Adv. Nucl. Phys. **16**, 1 (1986).
 - [3] J. Boguta and A. R. Bodmer, Nucl. Phys. **A292**, 413 (1977).
 - [4] D.P. Menezes and C. Providência, Phys. Rev. **C 68**, 035804 (2003).
 - [5] S.S. Avancini and D.P. Menezes, Phys. Rev. C **74**, 015201 (2006).
 - [6] N. Ashcroft, N.D. Mermim, Solid State Physics, Saunders College Publishing, Orlando, 1976
 - [7] L. D. Landau and E. M. Lifshitz, Statistical Physics, Pergamon Press, 1959.
 - [8] N. K. Glendenning and S. Moszkowski, Phys. Rev. Lett. **67**, 2414 (1991).
 - [9] N. K. Glendenning, Compact Stars, Springer-Verlag, New-York, 2000.
 - [10] F.X. Timmes and D. Arnett, Astrophys. J. Suppl. **125**, 277 (1999).
 - [11] J.M. Lattimer and F.D. Swesty, Nucl. Phys. **535**, 331 (1991).
 - [12] D. G. Ravenhall, C. J. Pethick, and J. R. Wilson, Phys. Rev. Lett. **50**, 2066 (1983); M. Hashimoto, H. Seki, and M. Yamada, Prog. Theor. Phys. **71**, 320 (1984).
 - [13] G. Watanabe, K. Sato, K. Yasuoka, and T. Ebisuzaki, Phys. Rev. C **69**, 055805 (2004); G. Watanabe, T. Maruyama, K. Sato, K. Yasuoka, and T. Ebisuzaki, Phys. Rev. Lett. **94**, 031101 (2005).
 - [14] T. Maruyama, T. Tatsumi, D. N. Voskresensky, T. Tanigawa, and S. Chiba, Phys. Rev. C **72**, 015802 (2005).
 - [15] H. Shen, H. Toki, K. Oyamatsu, K. Sumiyoshi, Nucl. Phys. **A 637**, 435 (1998); H. Shen, H. Toki, K. Oyamatsu, K. Sumiyoshi, *User Notes for Relativistic EoS Tables*.
 - [16] K. Sumiyoshi, H. Kuwabara, H. Toki, Nucl. Phys. **A 581**, 725 (1995).
 - [17] D.P. Menezes and C. Providência, Phys. Rev. **C 68**, 035804 (2003); A.M.S. Santos and D.P. Menezes, Phys. Rev. **C 69**, 045803 (2004).

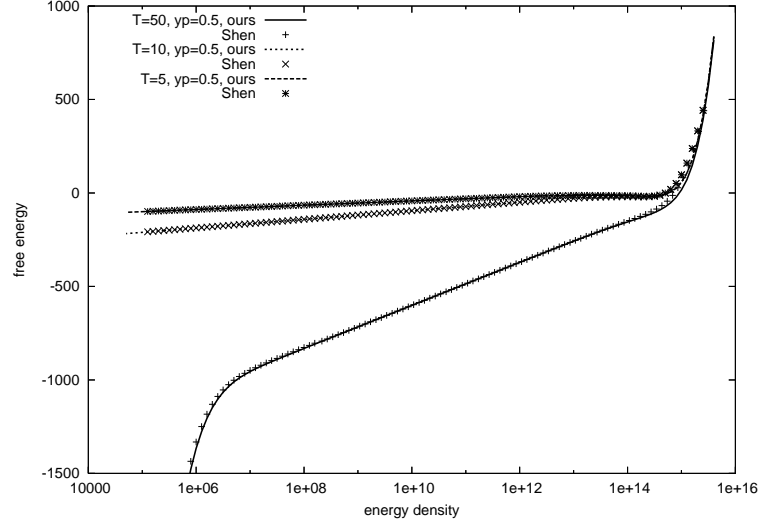
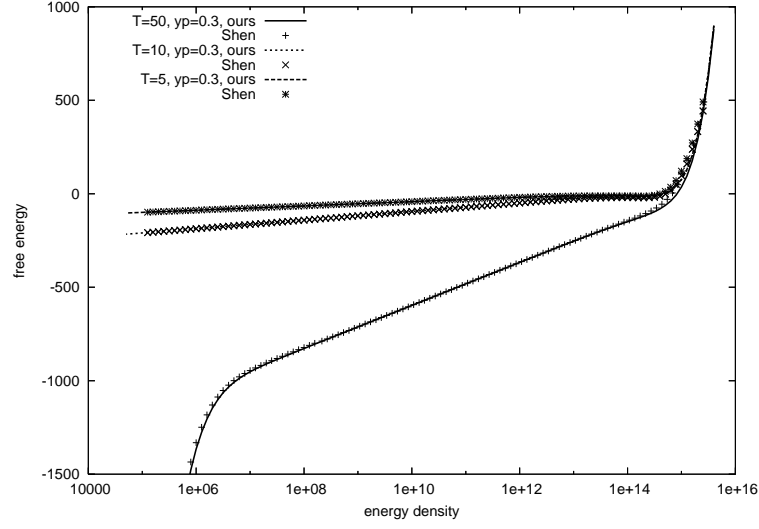
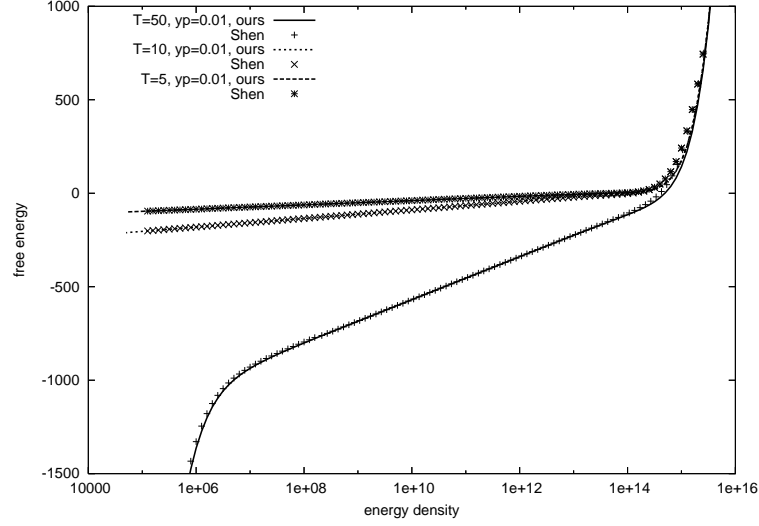
$y_p=0.5$

 $y_p=0.3$

 $y_p=0.01$


FIG. 1: Free energy (MeV/fm³) as function of the energy density (g/cm³) for different temperatures (MeV).

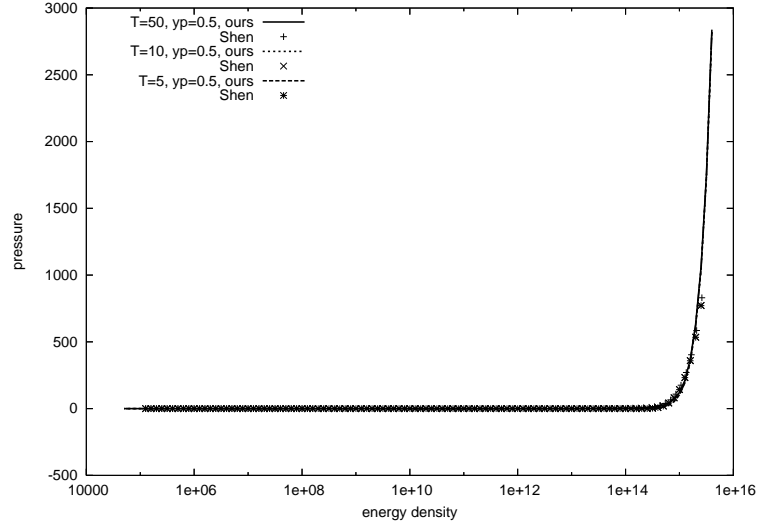
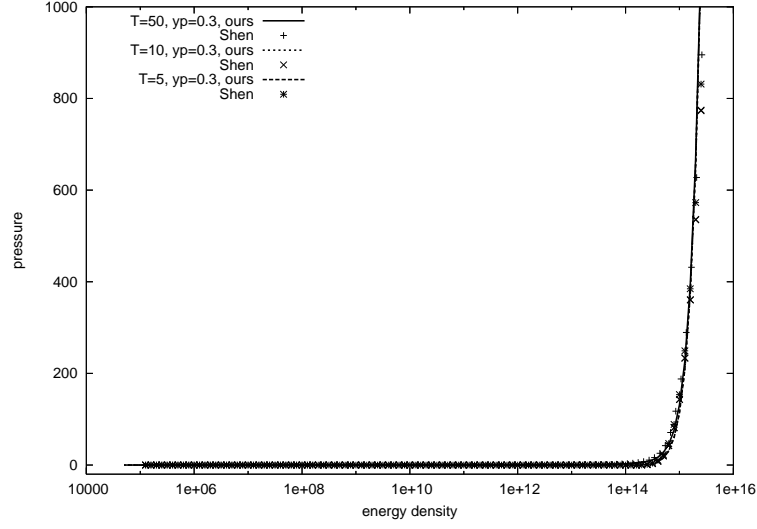
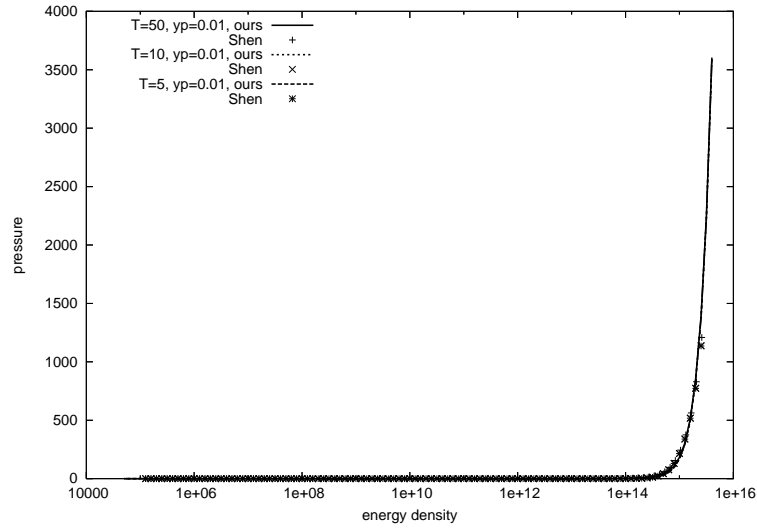
$y_p=0.5$

 $y_p=0.3$

 $y_p=0.01$


FIG. 2: Pressure (MeV/fm³) as function of the energy density (g/cm³) for different temperatures (MeV).

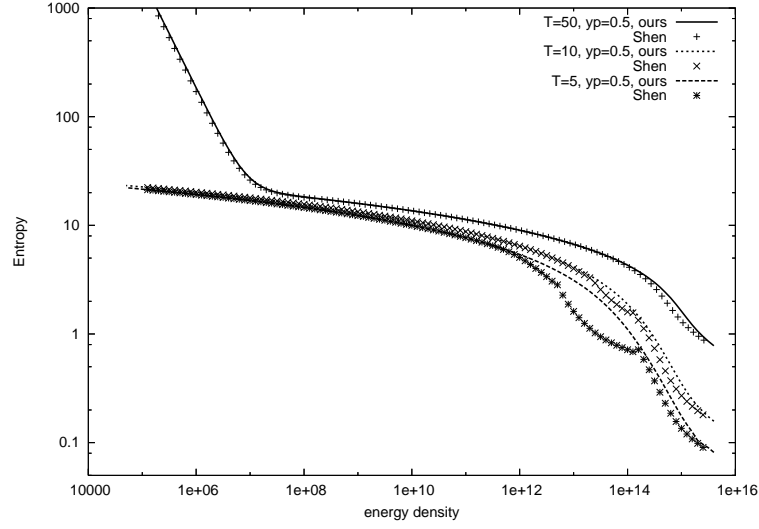
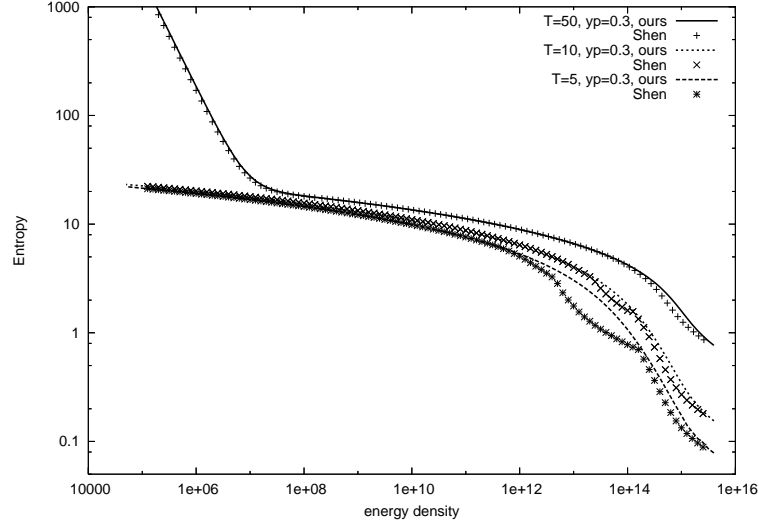
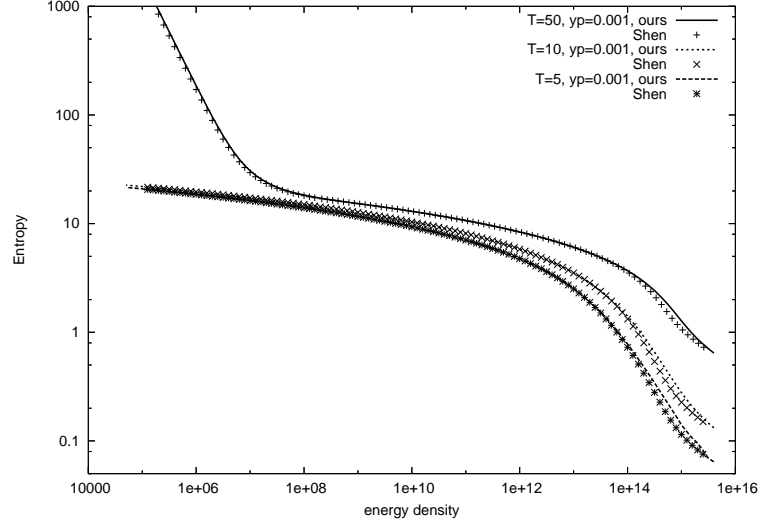
$y_p=0.5$

 $y_p=0.3$

 $y_p=0.01$


FIG. 3: Entropy per baryon as function of the energy density (g/cm^3) for different temperatures (MeV).

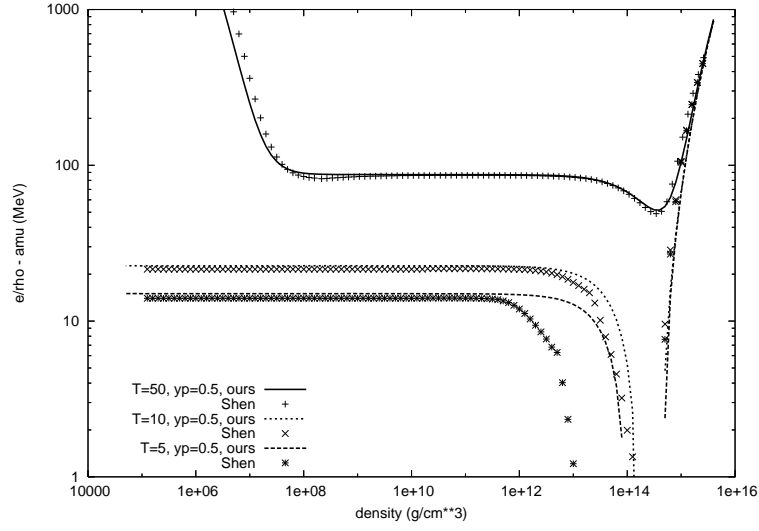


FIG. 4: Internal energy of symmetric matter for different temperatures.

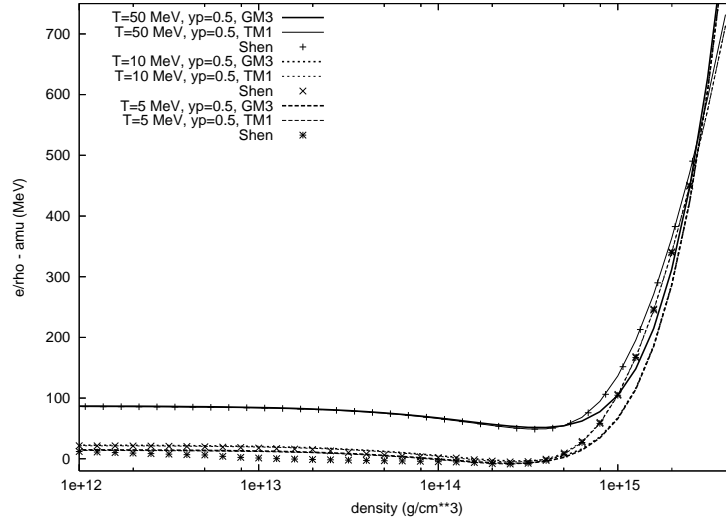


FIG. 5: Internal energy of symmetric matter for different temperatures for homogeneous matter within GM3 and TM1 parametrizations, and the EoS of [15].